



Correlation between conduction velocity and frequency analysis in patients with atrial fibrillation using high-density charge mapping

Lam Dang¹ · Nathan Angel² · Min Zhu² · Jean-Marc Vesin³ · Christoph Scharf⁴

Received: 30 January 2022 / Accepted: 22 August 2022 / Published online: 6 September 2022
© International Federation for Medical and Biological Engineering 2022

Abstract

Spectral analysis of atrial signals has been used to identify regions of interest in atrial fibrillation (AF). However, the relationship to the atrial substrate is unclear. In this study, we compare regions with dominant frequency (DF), simultaneously determined in the left atrium (LA) by a novel noncontact mapping system using unipolar charge density signals, to the zones of slow conduction (SZ) during AF.

In 19 AF patients the conduction during AF was assessed by a validated algorithm and SZ compared to the DF and the DF ratio between the DF peak and the area under the total spectrum (DFR). The results were compared in five different regions of the LA. The reproducibility of SZ location at different time measurements was higher than for DF or DFR. The SZs are mainly confined at the anterior and posterior wall of the LA. There was no statistically significant correlation between SZ and DF or DFR across the atrium.

Keywords Atrial fibrillation · Noncontact mapping · Charge density · Zone of slow conduction · Spectral analysis

1 Introduction

Spectral analysis of atrial fibrillation (AF) signals has been used to identify regions of interest in patients with persistent atrial fibrillation after pulmonary vein isolation and areas with dominant frequency (DF) were thought to be drivers of persistent AF [1]. However, initial studies were done with sequential contact mapping, which does not allow simultaneous DF mapping in the entire atrium. In addition, the correlation of DF to other physiologic measures of atrial disease, such as conduction velocity in AF is unknown.

Noncontact potentials have been recorded by noncontact multielectrode catheters (the EnSite™ Array™) for simultaneous frequency analysis in the entire atrium [2]. However, the results have not been reproducible, which might be

related to the fact that unipolar voltage signals include the electrical far field signal [3].

Therefore, in order to decrease the far field component during DF analysis with noncontact mapping, we used a newly developed noncontact mapping system (AcQMap®, Actus Medical, Inc.). This system computes the source of the electrical field (potential), which is the charge density (CD=Coulomb/cm²) at the heart wall [4–6]. This is the first study reporting results of DF analysis from simultaneously obtained charge signals of the entire atrium.

First studies have been published reporting patterns of AF propagation waves in the entire atrium including automatic detection of areas with repeated focal discharges, rotational activities and local irregular conduction characteristics [7–9]. In addition, recently a new algorithm computing conduction velocity has been implemented in the system in order to determine the zones of slow conduction (SZ, slow zones, [10]). This is the first study to report the localization and reproducibility of SZ in the human atrium during AF.

Previous studies suggest that conduction velocity disturbances might play a role in arrhythmogenic substrate [11, 12]. The study from Grossi et al. shows correlation between bipolar signals and frequency during sinus rhythm and incremental pacing [13].

✉ Lam Dang
lam.dang.ch@gmail.com

¹ HerzGefässStiftung, Klinik im Park, Zurich, Switzerland

² Actus Medical, Inc, CA 92008 Carlsbad, USA

³ Applied Signal Processing Group, Swiss Federal Institute of Technology, Lausanne, Switzerland

⁴ Rhythmologie-Zürich AG, Zurich, Switzerland

This study was conducted to test the hypothesis that high frequency areas might be correlated to zones of SZ. In addition, the reproducibility of DF and SZ analysis in the human atrium was assessed during AF.

2 Methods

2.1 Electrophysiologic study and recording

Signal recordings from 19 patients during AF mapping under general anesthesia were used for offline analysis. All patients have given informed written consent for the study. Patient characteristics are summarized in Table 1. Antiarrhythmic drug treatment was stopped at

Table 1 Clinical characteristics of patients

	Paroxysmal AF (<i>n</i> =4)	Persistent AF (<i>n</i> =12)	Long-standing AF (<i>n</i> =3)
Male, %	2 (50)	8 (66.6)	3 (100)
Age	68±9	67±10	59±3
EF	58±9	58±5	59±3
LA mm	43±7	44±7	46±4
Previous PVI, %	4 (100)	7 (58)	0
S. heart disease	2	8	2
Hypertonic	1	7	0
Diabetes	1	1	0
Amiodarone	0	2	0

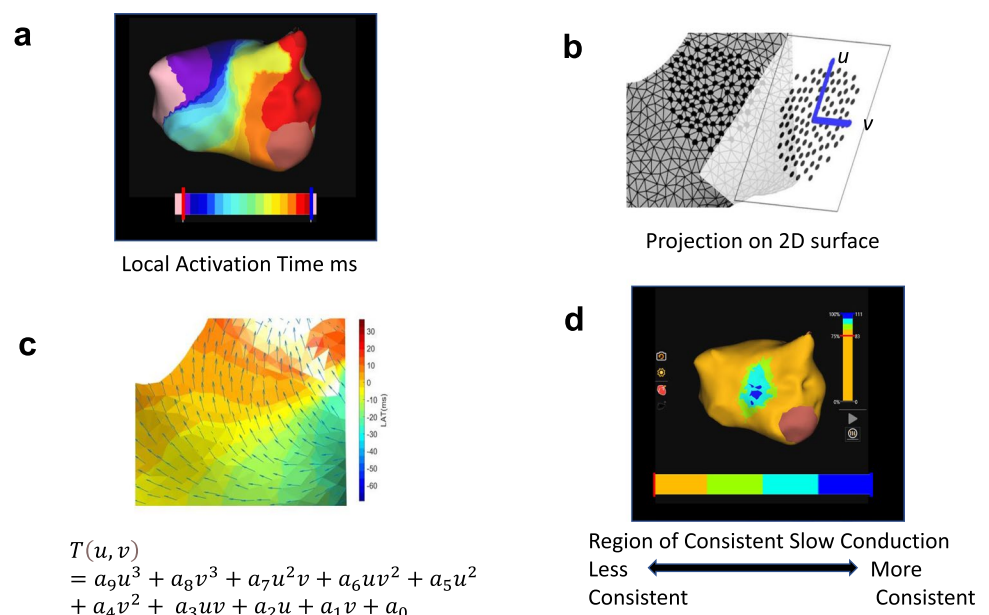
least 2 days before the procedure except for Amiodarone. After transeptal access, Heparin was administered until ACT was > 350 s. The AcQmap® catheter (Acutus Medical, Carlsbad, CA, USA) was deployed for anatomy reconstruction and unipolar electrogram recordings. The left atrium (LA) surface was meshed with triangular elements (> 3000 vertices, with a spatial resolution of ≈ 2 mm). Two baseline AF recordings of 30 s duration, which were at least 5 min apart, were used for analysis. In the patients with sinus rhythm, AF was induced by burst pacing. The unipolar voltage signals were filtered between 1 and 100 Hz for further processing.

2.2 Signal processing and data analysis

A) Localization of slow conduction zones

AF propagation history maps [14] of 10 s were computed for two segments at different recording times and were computed as previously described [15]. Then, propagation data were analyzed by the software algorithm for automatic location of slow conduction zones (SlowZone™ Locator (SZ), Acutus Medical, Carlsbad, CA, USA) (Fig. 1). Briefly, noncontact local activation times (LAT) are determined from the CD signals of the Acutus mapping system (Fig. 1a). At each vertex of the anatomical surface, a neighborhood (radius ≈ 5 mm) is defined and projected to a 2D surface (Fig. 1b) using the two first principal components (*u*, *v*) determined using a singular value decomposition. The conduction velocity is estimated using a 3rd order polynomial sur-

Fig. 1 SlowZone Locator Map (SZ Map). **a** Local activation time computed from CD. **b** 3D to 2D projection. For each vertex on the surface, define a neighborhood and project them to the 2 first principal components (*u* and *v*). **c** Compute conduction velocity with polynomial fit and project back to 3D anatomy. **d** SZ Map, regions with consistent slow conduction (in blue)



face fit [10, 16] to estimate the gradient of activation and inverted to estimate velocity on the mesh vertex (Fig. 1c). This estimation approach is similar to those implemented previously [10, 17, 18]. Single or multiple velocity maps can be combined to find regions of consistent slow conduction velocity (Fig. 1d). Zones of slow conduction were defined as having a conduction velocity magnitude < 0.3 m/s evaluated on a vertex basis, which is consistent with the literature [19–21].

B) Frequency analysis

At each vertex of the meshed surface, the unipolar CD signals during baseline AF were computed for the entire LA surface a sampling rate of 3125 Hz. The ventricular component of the unipolar raw signal was subtracted by the Acutus Mapping System, using a template-based method [22]. All data were exported for further analysis with MATLAB (Mathworks, Natick, MA, USA). A band-pass filter between 3 and 20 Hz was applied and the power spectrum estima-

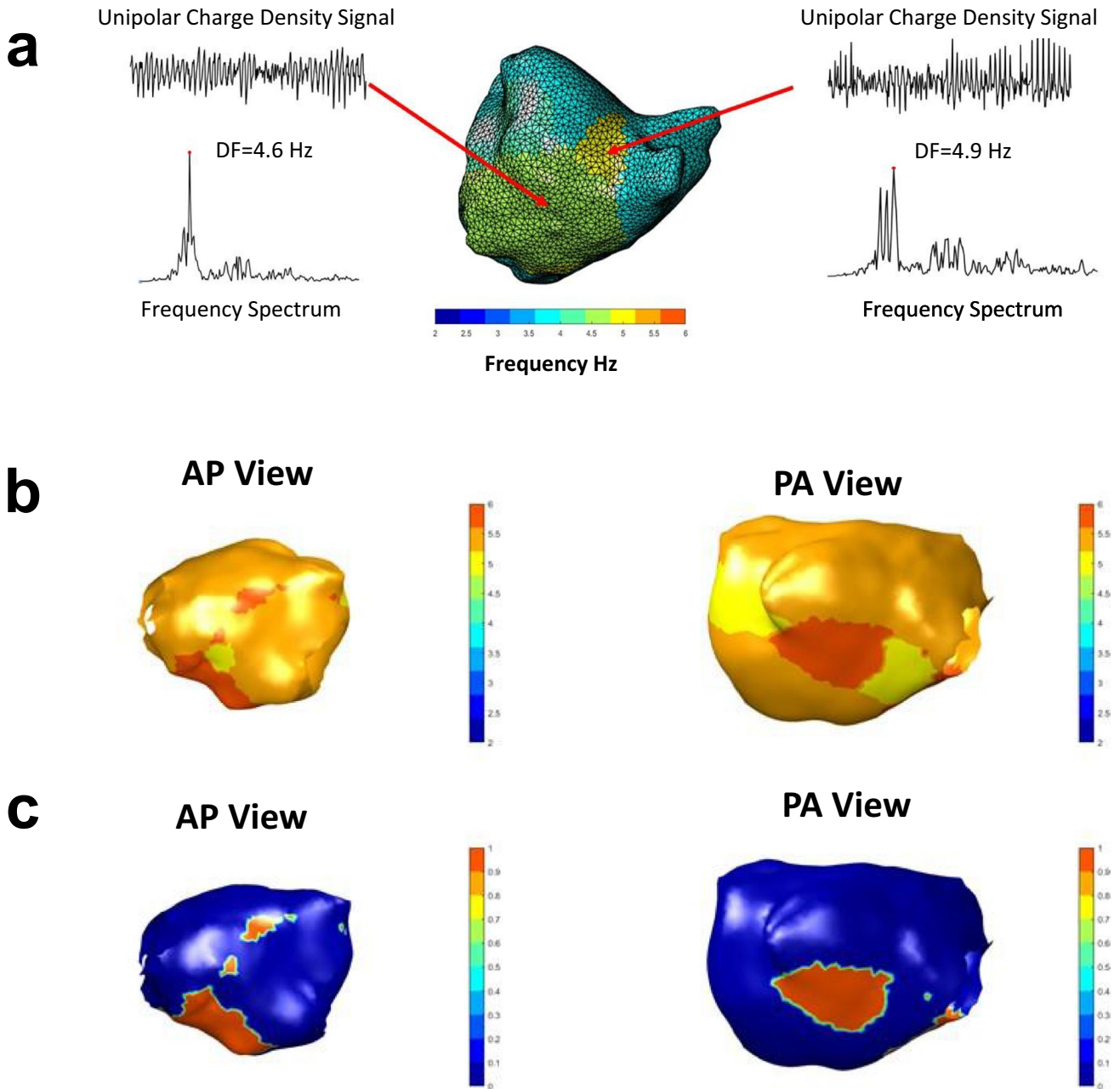
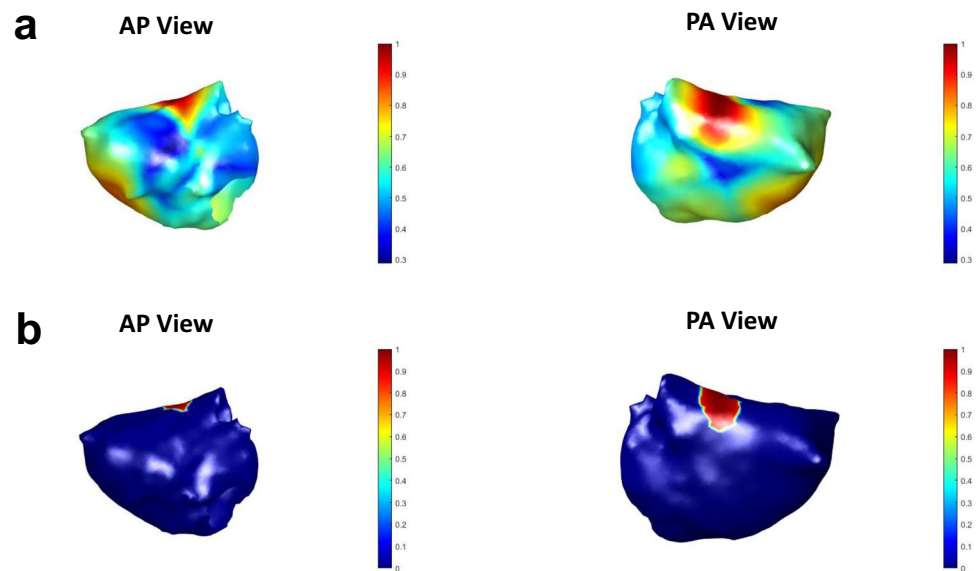


Fig. 2 **a** Dominant frequency (DF) computed at each vertex. **b** DF Map (frequency range from 2–6 Hz, blue to red). **c** DF regions was defined as $DF \geq 90\%$ of $DF_{MaxDFMap}$ (in red, binary map), where $DF_{MaxDFMap}$ was the maximum value of all DF withing the map (while the rest in blue).

Fig. 3 Dominant Frequency Ratio Map (DFR Map). **a** Ratio between dominant frequency (DF) peak and his total area of the spectrum (frequency value normalized between 0 and 1). **b** Region with DFR > 90% of DFR_{MaxMap} (in red, binary map)

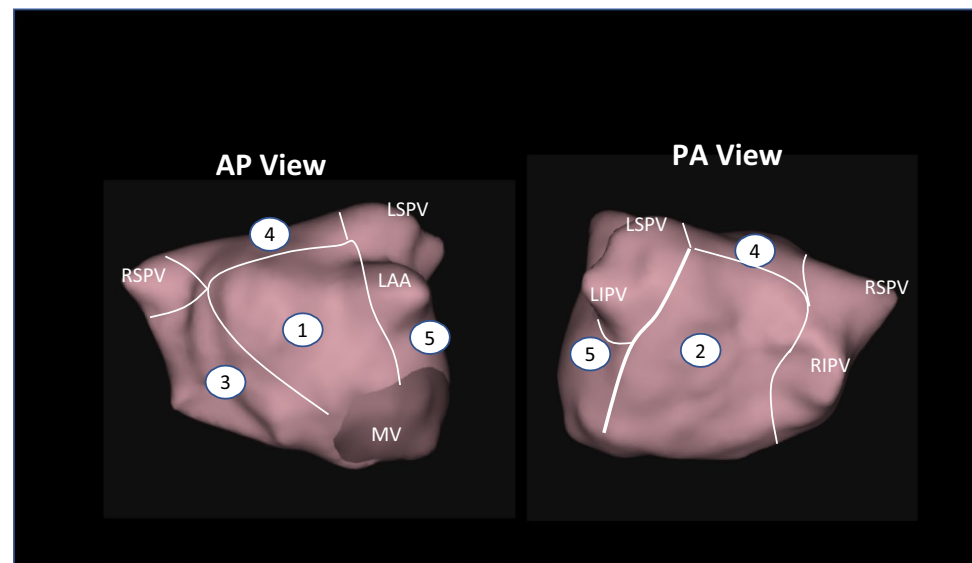


tion was performed using a smoothed periodogram (Hamming window) with a frequency resolution of 0.1 Hz [2]. For each individual vertex, the frequency spectrum was computed and the frequency with the highest power was taken as the dominant frequency (DF). Then, the DF values of each vertex were displayed in a color 3D map (Fig. 2a, b). As higher frequencies were not considered physiologic, the algorithm looks for DF below 20 Hz. All maps were visually inspected, especially in regions with abrupt change in frequencies and if harmonics were found, the fundamental frequency was used as DF. The region of high frequency activity was defined by a

DF larger than 90% of maximum DF in the entire LA ($DF_{MaxDFMap}$), (Fig. 2c) [23].

In addition, the relationship between the DF and the entire frequency spectrum was assessed for each vertex. The DF peak value was divided by the integral of the entire frequency spectrum, resulting DFR Ratio, which is a measure for the dispersion of the frequency spectrum and was visualized by a RF ratio Map (DFR), (Fig. 3a) as described previously [24, 25]. High DFR regions were defined by highest DFR, larger than 90% of $DFR_{MaxDFMap}$, where $DFR_{MaxDFMap}$ was the maximum DFR value of the entire map (Fig. 3b).

Fig. 4 Left Atrium Region: 1. Anterior Wall, 2 Posterior Wall, 3. Septum, 4. Roof, 5. Lateral Wall. MV = Mitral Valve, LAA = Left atrial appendage, LSPV = Left pulmonary veins, LIPV = Left inferior pulmonary, RSPV = Right superior pulmonary vein, RIPV = Right inferior pulmonary vein



C) Distribution of SZ, DF and DFR on the LA surface

Two SZ, DF, and DFR maps of 10 s recording each were constructed during baseline AF for each patient. The left atrium was arbitrarily divided into five regions (R1 to R5): 1. Anterior Wall, 2. Posterior Wall, 3. Septum, 4. Roof, 5. Lateral Wall (Fig. 4). The presence or absence of SZ, DF, and DFR was reported as a binary variable for each anatomical region.

2.3 Statistical analysis

Continuous data are reported as mean ± SD. Cohen’s Kappa coefficient was calculated to compare the agreement between the two maps and assess the relationship between the methods SZ and DF as well as SZ and DFR. The comparison between baseline recordings was

computed using Fisher-exact test. Spearman’s Rho Coefficient was used to compare the temporal correlation between the two baseline recordings. Statistical analysis was performed using R Foundation.

3 Results

In each of the 19 patients, 2 recordings of baseline AF for 10 s have been used to compute the SZ, DF, and DFR maps, leading to a total of 114 maps.

The clinical characteristics of the patients are summarized in Table 1. The findings of the study are visualized in one patient as an example (Fig. 5): the SZ is predominant at septum and anterior part of the LA, the DF regions are located at the anterior, posterior and roof of the LA, while DFR are only located at the posterior wall.

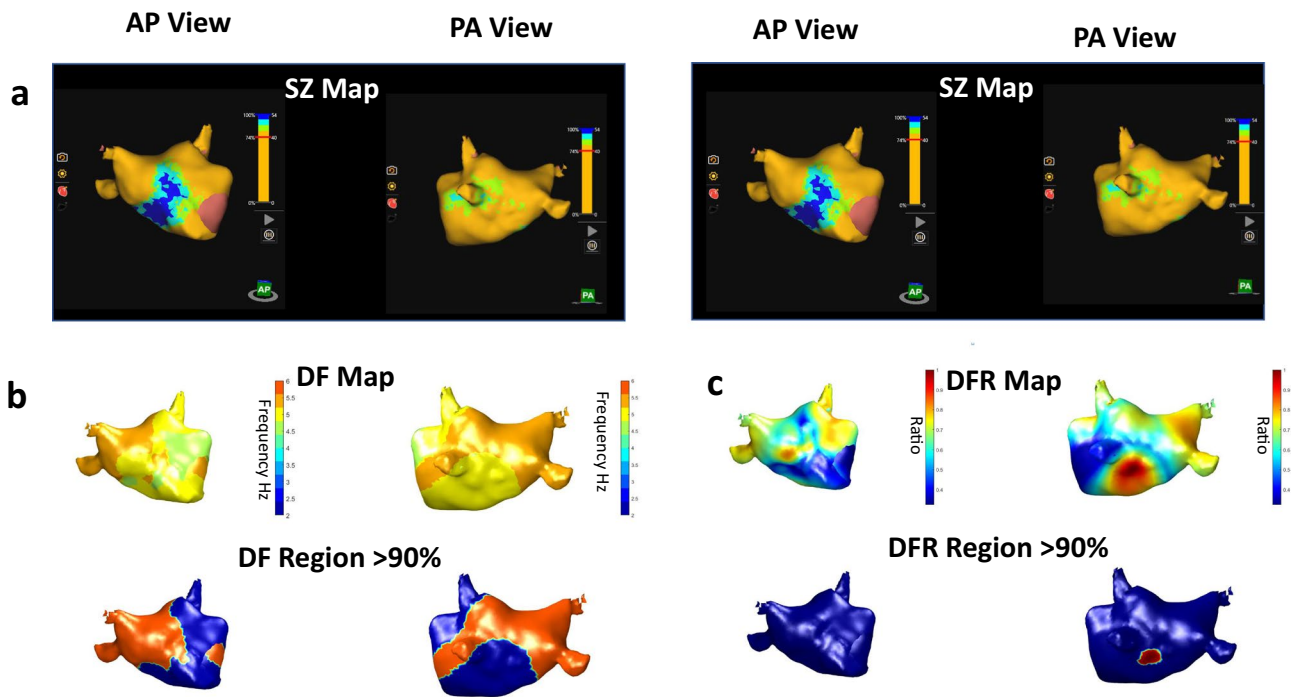


Fig. 5 Example of SZ, DF and DFR Maps. **a** SZ Map (in blue are regions with conduction velocity < 0.3 m/s) **b** DF Map and the region with 90% > DFMaxDFMap (in red) and **c** DFR Map and the region with 90% > DFRMaxMap (in red)

Table 2 Comparison between baseline 1 and baseline 2 for each analysis (slow zone (SZ), dominant frequency (DF) and dominant frequency ratio (DFR). R1 to R5 are the 5 different regions of the LA. Spearman’s Rho coefficient and *p*-value are reported

	R1 (Ant. wall)	R2 (Post. wall)	R3 (Septum)	R4 (Roof)	R5 (Lat. wall)
SZ1 vs SZ2	Rho=0.58 <i>p</i> =0.01	Rho=0.47 <i>p</i> =0.04	Rho=0.42 <i>p</i> =0.07	NA	Rho=−0.06 <i>p</i> =0.82
DF1 vs DF2	Rho=0.06 <i>p</i> =0.82	Rho=0.26 <i>p</i> =0.28	Rho=0.30 <i>p</i> =0.22	Rho=0.30 <i>p</i> =0.22	Rho=0.01 <i>p</i> =0.96
DFR1 vs DFR2	Rho=−0.015 <i>p</i> =0.95	Rho=0.23 <i>p</i> =0.34	Rho=0.07 <i>p</i> =0.77	Rho=−0.02 <i>p</i> =0.95	Rho=0.32 <i>p</i> =0.18

Table 3 Prevalence of slow zone (SZ), dominant frequency (DF) and dominant frequency ratio (DFR) for each LA region (R1–R5)

	R1 (Ant. wall)	R2 (Post. wall)	R3 (Septum)	R4 (Roof)	R5 (Lat. wall)
SZ1	29(76.3%)	21(55.3%)	13(34.2%)	0(0%)	2(5.3%)
DF	19(50.0%)	17(55.3%)	19(50.0%)	19(50.0%)	15(60.5%)
DFR	9(23.7%)	23(60.5%)	10(26.3%)	9(23.7%)	5(13.2%)

3.1 Temporal reproducibility

The temporal reproducibility between the two recordings (Table 2) was better for the location of the SZ (best value $\text{Rho}=0.58$, at the anterior wall) than for the DF analysis ($\text{Rho}=0.3$, at the roof) between the two maps. For the DFR analysis, the highest agreement was found on the lateral wall ($\text{Rho}=0.32$).

3.2 Slow conduction zones

The occurrence of SZ for each region is reported in Table 3 as percentage of the total 38 maps. Zones of slow conduction <0.3 m/s were found all but one map, they were more frequently in the anterior wall of patients and posterior wall in 76.3% of the maps than on the septum or posteriorly.

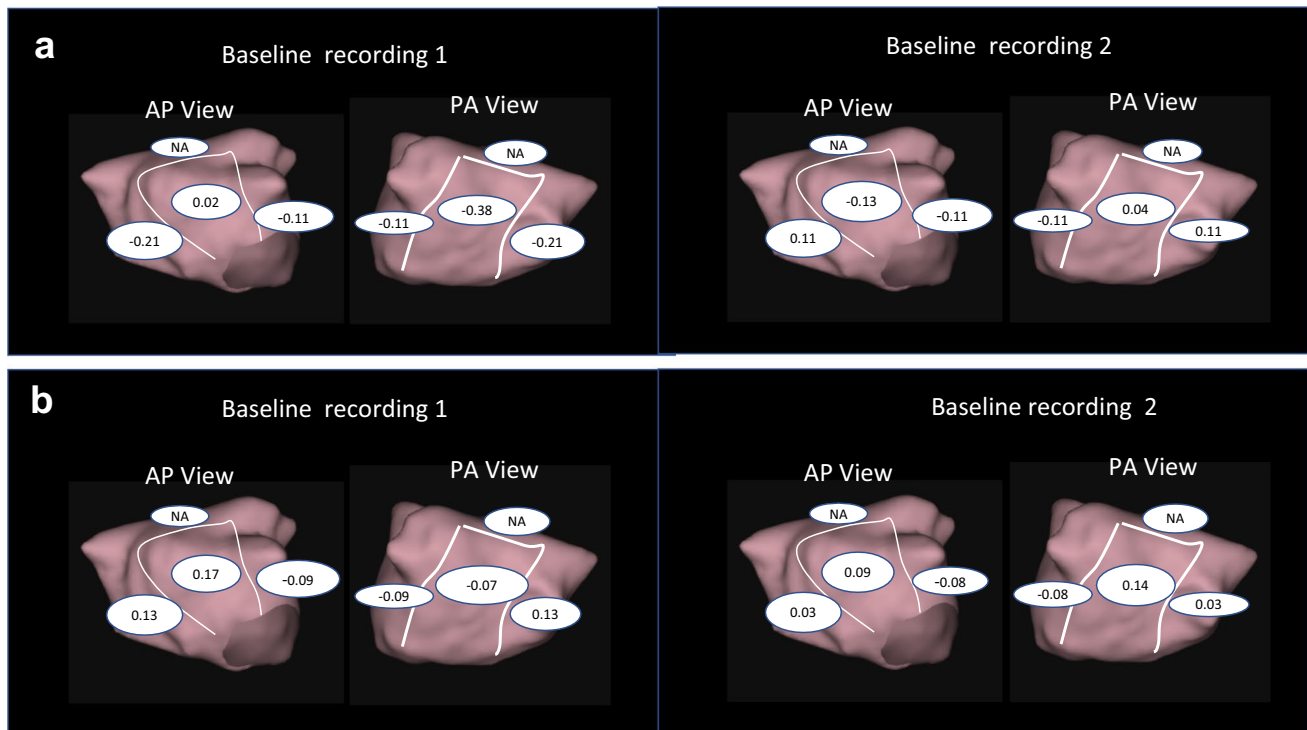
Interestingly the roof showed never zones of slow conduction. DF analysis does not show a clear localization of high frequency, while DFR method is mainly located at the posterior wall (60.5%).

3.3 Spectral analysis

In contrast, the DF was distributed all over the atrial regions (Table 3), as well as the highest DF ratio. The mean DF value of all LA sites did not differ between paroxysmal and persistent AF patients (5.2 ± 0.4 Hz versus 5.5 ± 0.8 Hz, $p=0.34$). While a significant mean DF value was observed between paroxysmal and long-standing AF patients (5.2 ± 0.4 Hz versus 6.1 ± 0.1 Hz, $p=0.0007$).

3.4 Agreement between slow conduction and frequency analysis

There was no significant agreement between the location of SZ and the location of DF or DFR, for both baseline recordings. Cohen's Kappa, K between -0.37 and 0.17 for SZ vs DF and K between -0.13 and 0.13 for SZ vs DFR (Fig. 6a for DF and Fig. 6b for DFR). Using a mixed model regression analysis to compare the SZ vs DF and SZ vs DFR, not significant correlation was obtained ($p > 0.21$).

**Fig. 6** Comparison between slow zone (SZ), dominant frequency (DF) and dominant frequency ratio (DFR) for each region at baseline 1 and baseline 2 recordings. Cohen's Kappa coefficient (K) for each

region is reported. **a** SZ vs DF for baseline 1 and 2. **b** SZ vs DFR for baseline 1 and 2

4 Discussion

This is the first study to report frequency analysis of CD signals simultaneously recorded in the entire atrium and to compare results to SZ during AF in humans.

4.1 Frequency analysis

This study shows that DF and DFR were not reproducible over time. For the five regions of the LA analyzed, no correlation has been observed between the first and second recordings ($p > 0.05$) (Table 2). This result agrees with previous findings [2, 3], where mappings were performed using unipolar noncontact voltage and bipolar contact electrograms. The DF analysis also shows a quasi-uniform distribution of the DF over the entire atrium. Only on the posterior wall that a higher occurrence of DF location was observed (Table 2). There was no significant difference in the mean DF values of all LA sites between paroxysmal and persistent AF patients (5.2 ± 0.4 Hz versus 5.5 ± 0.8 Hz, $p = 0.34$), as observed by Jarman et al. [2] and no significant correlation has been found between locations of DF and DFR. Frequency analysis has been performed widely. For bipolar voltage signals, hopeful results have been published initially [1], however the clinical value has been low because of poor reproducibility of sequential measurements of bipolar contact signals. Also, for noncontact unipolar voltage signals, several studies report mixed results, which were obtained by using a definition for frequency regions by 20% higher frequency than neighborhood points [2]. However, with that definition, we would only obtain the border of high frequency regions but not identify the spots with the DF itself.

Frequency analysis has not gained widespread clinical application because of inherent limitations of reproducibility [3, 26, 27] and lack of pathophysiological correlation to clinical characterizations to the atrial substrate.

4.2 Location of slow zones

There are no previous studies identifying zones of slow conduction in the human atrium during AF, because the technology was not available in other mapping systems. First, the reproducibility of the methods was tested, which showed that only the localization of SZ areas is somewhat reproducible in the anterior and posterior wall with moderate but significant correlation values ($Rho = 0.58$, $p = 0.01$ and $Rho = 0.47$, $p = 0.04$, respectively) (Table 2). Previous studies have shown that atrial conduction velocity has been correlated to arrhythmogenic substrate [28–31]. In Heida et al. [29], patients with a history of AF had slower conduction velocity (CV) at the Bachmann's bundle region compared to a control group, and Zhen et al. study [28] shows slow CV at the septum and anterior wall. This study also

confirmed that SZ region are mainly confined at the anterior wall of the LA as reported by Kurato et al. [30]. For each of the 19 patients, 2 maps of SZ have been computed. Among these 38 maps, 29 maps were found having SZ at the anterior wall (76.3%) and 21 maps with SZ at the posterior wall (55.3%) (Table 3). Interestingly, no SZ have been found on the roof, this might be due to the small population included in this study.

The analysis of atrial CV is a new tool and might be more representative for the atrial substrate, because it is more reproducible, has been validated against contact measurements of CV [10] and represents a clinical meaningful value of atrial electrical properties. Whether the cutoff value of 3 m/s as used in the literature translates into prognostic information has to be determined by future studies. Also, the correlation of CV during various rhythms (sinus rhythm, pacing, flutter, fibrillation) has to be determined to further characterize the impact of functional alterations of the atrial substrate.

4.3 Relationship between frequency analysis, slow zones and complex fractionated atrial electrograms

This is the first study to compare DF and SZ. Our results did not show agreements between location of DF and SZ or DFR and SZ. This is not surprising since results of DF and DFR were not stable over time. One study reports a strong correlation between CV and the barycenter of the frequency spectrum Grossi et al. [13]. The study was performed during incremental pacing, and CV was computed along the catheter inserted along the coronary sinus. So, a comparison to our current study would not be relevant, since they used different technology and spectrum analysis during pacing.

Previous studies have investigated the relationship between DF and complex fractionated electrograms (CAFÉ) using bipolar signals [32, 33] in patient presenting for AF ablation. Habel et al. mapped the left atrium using a 64-electrode basket catheter while Vermal et al. [33] used a circular mapping catheter during persistent AF patient. These studies did not show a significant correlation between sites of high frequency and CAFÉs, as well as their stability over time. From these studies, no conclusion to guide RFA could be drawn.

4.4 Methodological discussion

In the current study, the time segment used to compute DF and map of SZ was arbitrarily chosen at 10 s. The choice was made based on the processing capacity of the software to compute larger map duration. The AcQMap® allows to compute the SZ in different manners: (a) using Supermap recording, which is a specific mode to acquire data by

rowing the AcQMap® catheter in the atrium, resulting in a single map based on a large set of non-contact electrogram recordings, (b) using a combination of several propagation maps recorded, and (c) using a single map recording. Since we had 10 s of recording for each map, we used only one map of 10 s to compute the SZ map. During 10 s of AF, at each vertex, CVs were computed for each activation detected. Atrial region with > 75% of the CVs below 0.3 m/s were displayed as SZ, which are standard settings of the AcQMap® algorithm. The size of the SZ was also not reported in this study, only their localization. The time interval between each map was approximately 5 min, the effect of this parameter on the map was not accessed in this study. The current AcQmap® software was not also considering the magnitude of the signal to compute the zone of slow conduction, which might also play a role.

5 Limitations

The present study includes a small patient group; however, the amount of data collected are considerable. Two baselines AF recordings of 10 s each and data are analyzed over 3000 vertices for each anatomy. Novel and meaningful findings of statistical significance were obtained. Therefore, it is doubtful that different results would appear with larger patient numbers. Another limitation is that the size of LA was not computed, and inaccuracy can be introduced if the distance from the center of the noncontact catheter to the wall is > 4 cm. However, the mean value of left atrial diameter was 4.3 cm and the largest diameter 5.9 cm. Finally, further follow-up studies are necessary to address the clinical impact of our findings.

6 Conclusion

In this study, the locations of SZ and DF do not match in AF patients. The SZ are mainly confined at the anterior and posterior wall of the LA. The consistency of the results over time is only given for SZ and not for the spectral analysis. These findings suggest that the SZ, but not the DF could be used for comparison to measures of the atrial substrate.

Glossary AF: Atrial fibrillation; CAFE: Complex fractionated electrogram; CD: Charge density ($C\text{-cm}^{-2}$); CV: Conduction velocity ($\text{m}\cdot\text{s}^{-1}$); SZ: Slow zone; LAT: Local activation time (ms); FFT: Fast Fourier transform; DF: Dominant frequency (Hz); DFR: Dominant frequency ratio, the ratio between the DF peak and the area under the total spectrum; LA: Left atrium; MV: Mitral valve; LSPV: Left pulmonary vein; LIPV: Left inferior pulmonary vein; RSPV: Right superior pulmonary vein; RIPV: Right inferior pulmonary vein; LAA: Left atrial appendage

Declarations

Drs Dang and Scharf are co-founder and shareholders of Acutus Meical Inc.
Drs Angel and Zhu were previously employees and shareholders of Acutus Medical Inc.
Dr Vesin has no disclosure.

References

- Sanders P, Berenfeld O, Hocini M, Jaïs P, Vaidyanathan R, Hsu L-F, Garrigue S, Takahashi Y, Rotter M, Sacher F, Scavée C, Ploutz-Snyder R, Jalife J, Haïssaguerre M (2005) Spectral analysis identifies sites of high-frequency activity maintaining atrial fibrillation in humans. *Circulation* 112(6):789–797
- Jarman JWE, Wong T, Kojodjojo P, Spohr H, Davies JE, Roughton M, Francis DP, Kanagaratnam P, Markides V, Davies DW, Peters NS (2012) Spatiotemporal behavior of high dominant frequency during paroxysmal and persistent atrial fibrillation in the human left atrium. *Circ Arrhythmia electrophysiol* 5(4):650–658
- Schuessler RB, Kay MW, Melby SJ, Branham BH, Boineau JP, Damiano RJ (2006) Spatial and temporal stability of the dominant frequency of activation in human atrial fibrillation. *J Electrocardiol* 39:S7–S12
- Grace A, Willems S, Meyer C, Verma A, Heck P, Zhu M, Shi X, Chou D, Dang L, Scharf C, Scharf G, Beatty G (2019) High-resolution noncontact charge-density mapping of endocardial activation. *JCI insight* 4(6)
- Shi R, Parikh P, Chen Z, Angel N, Norman M, Hussain W, Butcher C, Haldar S, Jones DG, Riad O, Markides V, Wong T (2020) Validation of dipole density mapping during atrial fibrillation and sinus rhythm in human left atrium. *JACC. Clinical electrophysiology* 6(2):171–181
- Gagyí RB, Noten AME, Lesina K, Mahmoodi BK, Yap S-C, Hoogendijk MG, Wijchers S, Bhagwandien RE, Szili-Torok T (2021) New possibilities in the treatment of brief episodes of highly symptomatic atrial Tachycardia: the usefulness of single-position single-beat charge density mapping. *Circ Arrhythmia and electrophysiol* 14(11):e010340
- Pope MTB, Kuklik P, Gala ABE, Leo M, Mahmoudi M, Paisey J, Betts TR (2021) Spatial and temporal variability of rotational, focal, and irregular activity: practical implications for mapping of atrial fibrillation. *J Cardiovasc Electrophysiol* 32:2393–2403
- Pope MTB, Kuklik P, Gala ABE, Leo M, Mahmoudi M, Paisey J, Betts TR (2022) Impact of adenosine on wavefront propagation in persistent atrial fibrillation: insights from global non-contact charge density mapping of the left atrium. *J Am Heart Assoc: Cardiovasc Cerebrovasc Dis* 11
- Shi R, Chen Z, Butcher C, Zaman JA, Boyalla V, Wang YK, Riad O, Sathishkumar A, Norman M, Haldar S, Jones DG, Hussain W, Markides V, Wong T (2020) Diverse activation patterns during persistent atrial fibrillation by noncontact charge-density mapping of human atrium. *J arrhythmia* 36(4):692–702
- Mickelsen SR, Angel N, Shah P, Shi X, Chou D (2021) B-PO05-085 Regional conduction velocity measurements: comparing contact and non-contact activation techniques. *Heart Rhythm* 18:S406
- Pytkowski M, Jankowska A, Maciag A, Kowalik I, Sterlinski M, Szwed H, Saumarez RC (2008) Paroxysmal atrial fibrillation is associated with increased intra-atrial conduction delay. *Europace* 10:1415–1420

12. Zheng Y, Xia Y, Carlson J, Kongstad O, Yuan S (2017) Atrial average conduction velocity in patients with and without paroxysmal atrial fibrillation. *Clin Physiol Funct Imaging* 37:596–601
13. Grossi S, Grassi F, Galleani L, Bianchi F, SibonaMasi A, Conte MR (2016) Atrial conduction velocity correlates with frequency content of bipolar signal. *Pacing clin electrophysiol : PACE* 39(8):814–821
14. Grace A, Verma A, Willems S (2017) Dipole density mapping of atrial fibrillation. *Eur heart j* 38(1):5–9
15. Willems S, Verma A, Betts TR, Murray S, Neuzil P, Ince H, Steven D, Sultan A, Heck PM, Hall MC, Tondo C, Pison L, Wong T, Boersma LV, Meyer C, Grace A (2019) Targeting nonpulmonary vein sources in persistent atrial fibrillation identified by noncontact charge density mapping: UNCOVER AF Trial. *Circulation. Arrhythmia electrophysiol* 12(7):e007233
16. Bayly PV, KenKnight BH, Rogers JM, Hillsley RE, Ideker RE, Smith WM (1998) Estimation of conduction velocity vector fields from epicardial mapping data. *IEEE trans bio-med eng* 45(5):563–571
17. Barnette AR, Bayly PV, Zhang S, Walcott GP, Ideker RE, Smith WM (2000) Estimation of 3-D conduction velocity vector fields from cardiac mapping data. *IEEE Trans Biomed Eng* 47(8):1027–1035
18. Good WW, Gillette KK, Zenger B, Bergquist JA, Rupp LC, Tate J, Anderson D, Gsell MAF, Plank G, MacLeod RS (2021) Estimation and validation of cardiac conduction velocity and wavefront reconstruction using epicardial and volumetric data. *IEEE Trans Biomed Eng* 68(11):3290–3300
19. Wong GR, Nalliah CJ, Lee G, Voskoboinik A, Prabhu S, Parameswaran R, Sugumar H, Anderson RD, McLellan A, Ling L-H, Morton JB, Sanders P, Kistler PM, Kalman JM (2019) Dynamic atrial substrate during high-density mapping of paroxysmal and persistent AF. *JACC: Clin Electrophysiol* 5:1265–1277
20. Honarbakhsh S, Schilling RJ, Orini M, Providencia R, Keating E, Finlay M, Sporton S, Chow A, Earley MJ, Lambiase PD, Hunter RJ (2019) Structural remodeling and conduction velocity dynamics in the human left atrium: relationship with reentrant mechanisms sustaining atrial fibrillation. *Heart Rhythm* 16:18–25
21. Konings KTS, Kirchhof CJHJ, Smeets JRLM, Wellens HJJ, Penn OC, Allessie MA (2000) High-density mapping of electrically induced atrial fibrillation in humans. Springer, Netherlands, pp 549–567
22. Ng J, Kadish AH, Goldberger JJ (2007) Technical considerations for dominant frequency analysis. *J cardiovasc electrophysiol* 18(7):757–764
23. Li X, Chu GS, Almeida TP, Vanheusden FJ, Salinet J, Dastagir N, Mistry AR, Vali Z, Sidhu B, Stafford PJ, Schlindwein FS, Ng GA (2021) Automatic extraction of recurrent patterns of high dominant frequency mapping during human persistent atrial fibrillation. *Front physiol* 12:649486
24. Everett TH, Kok LC, Vaughn RH, Moorman JR, Haines DE (2001) Frequency domain algorithm for quantifying atrial fibrillation organization to increase defibrillation efficacy. *IEEE trans bio-med eng* 48(9):969–978
25. Everett TH, Moorman JR, Kok LC, Akar JG, Haines DE (2001) Assessment of global atrial fibrillation organization to optimize timing of atrial defibrillation. *Circulation* 103(23):2857–2861
26. Kogawa R, Okumura Y, Watanabe I, Kofune M, Nagashima K, Mano H, Sonoda K, Sasaki N, Ohkubo K, Nakai T, Hirayama A (2015) Spatial and temporal variability of the complex fractionated atrial electrogram activity and dominant frequency in human atrial fibrillation. *J Arrhythmia* 31:101–107
27. Li X, Chu GS, de Almeida TP, Salinet J, Mistry AR, Vali Z, Stafford PJ, Schlindwein FS, Ng GA (2018) *Dominant frequency variability mapping for identifying stable drivers during persistent atrial fibrillation using noncontact mapping*. *Comput Cardiol*
28. Zheng Y, Xia Y, Carlson J, Kongstad O, Yuan S (2017) Atrial average conduction velocity in patients with and without paroxysmal atrial fibrillation. *Clin physiol funct imaging* 37(6):596–601
29. Heida A, van Schie MS, van der Does WFB, Taverne YJHJ, Bogers AJJC, de Groot NMS (2021) Reduction of conduction velocity in patients with atrial fibrillation. *J Clin Med* 10:2614
30. Kurata N, Masuda M, Kanda T, Asai M, Iida O, Okamoto S, Ishihara T, Nanto K, Tsujimura T, Matsuda Y, Hata Y, Mano T (2020) Slow whole left atrial conduction velocity after pulmonary vein isolation predicts atrial fibrillation recurrence. *J Cardiovasc Electrophysiol* 31:1942–1949
31. Frontera A, Pagani S, Limite LR, Peirone A, Fioravanti F, Enache B, Cuellar Silva J, Vlachos K, Meyer C, Montesano G, Manzoni A, Dedé L, Quarteroni A, Lațcu DG, Rossi P, Della Bella P (2022) Slow conduction corridors and pivot sites characterize the electrical remodeling in atrial fibrillation. *JACC Clin electrophysiol* 8(5):561–577
32. Verma A, Lakkireddy D, Wulffhart Z, Pillarisetti J, Farina D, Beardsall M, Whaley B, Giewercer D, Tsang B, Khaykin Y (2011) Relationship between complex fractionated electrograms (CFE) and dominant frequency (DF) sites and prospective assessment of adding DF-guided ablation to pulmonary vein isolation in persistent atrial fibrillation (AF). *J Cardiovasc Electrophysiol* 22(12):1309–1316
33. Habel N, Znojkwicz P, Thompson N, Müller JG, Mason B, Calame J, Calame S, Sharma S, Mirchandani G, Janks D, Bates J, Noori A, Karnbach A, Lustgarten DL, Sobel BE, Spector P (2010) The temporal variability of dominant frequency and complex fractionated atrial electrograms constrains the validity of sequential mapping in human atrial fibrillation. *Heart Rhythm* 7:586–593

Publisher's note Springer Nature remains neutral with regard to jurisdictional claims in published maps and institutional affiliations.

Springer Nature or its licensor holds exclusive rights to this article under a publishing agreement with the author(s) or other rightsholder(s); author self-archiving of the accepted manuscript version of this article is solely governed by the terms of such publishing agreement and applicable law.



Lam Dang graduated from the Swiss Federal Institute of Technology, Lausanne, Switzerland in 2001 with a Msc degree in Microengineering and a postgraduate degree in Biomedical Engineering. In 2006, he received his PhD degree in Biomedical Engineering in the domain of atrial arrhythmias using computer models. Then, he joined the Cardiovascular Center at Klinik im Park, Zürich, as clinical field specialist and continue his research in atrial

fibrillation. In 2010, he co-founded with Drs C.Scharf, G. Scharf and R. Werneth Acutus Medical Inc.



Nathan Angel was born in Fresno, CA, USA in 1988. He received his B.S and M.S degree in Biomedical Engineering from the California Polytechnic State University-San Luis Obispo, USA, in 2011 and his PhD degree in bioengineering from the University of Utah, USA in 2016. Dr Angel was employed as a scientist at Acutus Medical from 2016 to 2022.



Min Zhu was born in Shengzhou, Zhejiang, China in 1983. She received her B.S. in Mathematics and Applied Mathematics and M.S in Computing Mathematics in Zhejiang University, China in 2006 and 2008, respectively. She obtained her Ph.D. degree in Electrical and Computer Engineering from the University of Oklahoma in 2013. She joined Acutus Medical Inc. after her graduation and currently, she was holding the position of Director of Engineering, Algorithm until 2022.



Jean-Marc Vesin received the graduate degree from the Ecole Nationale Supérieure d'Ingénierus Electriciens de Grenoble (ENSIEG, Grenoble, France) in 1980. He received the MSc degree from Laval University, Québec City, Canada, in 1984, where he spent 4 years on research projects. After 2 years in the industry, he joined the Signal Processing Institute of the Swiss Federal Institute of Technology, Lausanne, Switzerland (EPFL), where he received the PhD degree in 1992. He currently heads the Applied Signal

Processing Group (ASPG) at EPFL. His main interests include biomedical signal processing, adaptive signal analysis, nonlinear signal modeling and analysis, and computer modeling of heart electrical activity. He has authored or coauthored more than 50 publications in peer-reviewed journals, as well as several book chapters.



Christoph Scharf received his MD degree from the University of Zürich in 1991. He obtained his FMH in internal Medicine and Cardiology (Swiss Board Certification) and completed his specialization in electrophysiology at the University of Michigan (Clinical fellowship and attending physician) under the supervision of Dr. Fred Morady. In 2010, he co-founded with Drs L. Dang, G. Scharf and R. Werneth Acutus Medical Inc. His is currently practicing at Hirslanden Clinic in Zürich, Switzerland.